Pointing LISA-like Gravitational Wave Detectors

Karan Jani[1,2,3], Lee Samuel Finn[1,3], Matthew Benacquista[4]

[1] Department of Astronomy and Astrophysics, Pennsylvania State University, University Park, PA 16802, [2] Current address: School of Physics, Georgia Institute of Technology, Atlanta, GA 30332- 0430,
[3] Department of Physics, Pennsylvania State University, University Park, PA 16802, [4] Center for Gravitational Wave Astronomy, The University of Texas at Brownsville, 80 Fort Brown, Brownsville, TX 78520

LISA-like Orbits

In order to detect low-frequency gravitational radiation (0.1-100 mHz), space-based detectors are necessary to avoid terrestrial seismic and gravity-gradient noise sources. Most current designs for such a detector are slight modifications of the classic LISA concept. Three spacecraft follow independent circumsolar orbits that lead or lag the Earth in its orbit by tens of degrees. The three spacecraft form a triangular constellation that is relatively stable and nearly equilateral. The plane of the constellation is inclined by 60° with respect to the ecliptic. The guiding center of the constellation orbits Sol at an AU, while the normal to the constellation plane precesses about the normal to the ecliptic, and the constellation orbits within the constellation plane. All of the motions occur with a period of 1 year, and are shown in Fig. 1.

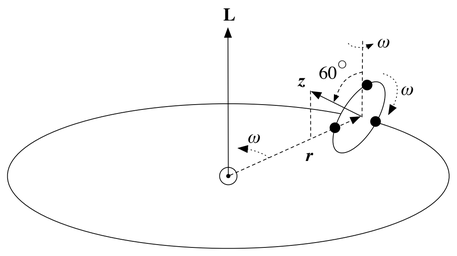

Figure 1: Schematic of the LISA constellation in orbit about Sol.

Detector Response

In the low-frequency (small antenna) limit, the response of LISA to a plane gravitational wave of the form

$$\boldsymbol{h} = h_+(t - \hat{\boldsymbol{n}}\cdot\boldsymbol{x})\boldsymbol{e}_+(\hat{\boldsymbol{n}}) + h_\times(t - \hat{\boldsymbol{n}}\cdot\hat{\boldsymbol{x}})\boldsymbol{e}_\times(\hat{\boldsymbol{n}}) \qquad (1)$$

may be expressed as

$$r(t) = \frac{L}{2}\left[F_+(\boldsymbol{n},t)h_+(t-\boldsymbol{n}\cdot\boldsymbol{x}_c) + F_\times(\boldsymbol{n},t)h_\times(t-\boldsymbol{n}\cdot\boldsymbol{x}_c)\right], \qquad (2)$$

where $\boldsymbol{x}_c$ is the location of the constellation guiding center, L is the effective arm-length,

$$F_+ = d_{ij}e^{ij}_+ \qquad F_\times = d_{ij}e^{ij}_\times, \qquad (3)$$

with the antenna projection tensor defined by:

$$\boldsymbol{d} = \boldsymbol{u}\otimes\boldsymbol{u} - \boldsymbol{v}\otimes\boldsymbol{v}. \qquad (4)$$

The vectors $\boldsymbol{u}$ and $\boldsymbol{v}$ are the unit vectors in the direction of the interferometer arms—see Fig. 2.

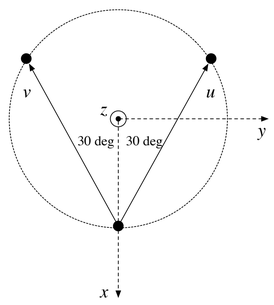

Figure 2: The LISA constellation and its rest frame coordinates. The unit vectors **u** and **v** define the antenna projection tensor. The four nulls lie in the $\pm x$ and $\pm y$ directions.

Sensitivity Measure

Our basic measure of LISA's sensitivity is the quadrature sum of F_+ and $F_\times$,

$$\frac{d\rho^2}{dt} = F_+^2(\boldsymbol{n},t) + F_\times^2(\boldsymbol{n},t). \qquad (5)$$

We can determine a normalized average value of ρ^2 by integrating over a year-long observation and normalizing so that the maximum value, over all $\boldsymbol{n}$, is unity:

$$\rho^2 = \int_0^{1\mathrm{yr}} \frac{d\rho^2}{dt}\,dt, \qquad \widehat{\rho^2}(\boldsymbol{n}) = \frac{\rho^2(\boldsymbol{n})}{\max_{\boldsymbol{n}'}\rho^2(\boldsymbol{n}')}. \qquad (6)$$

The dependence of ρ^2 on $\boldsymbol{n}$ is identical to the dependence on $\boldsymbol{n}$ of the power signal-to-noise associated with a compact object binary system when averaged over the binary's orientation.

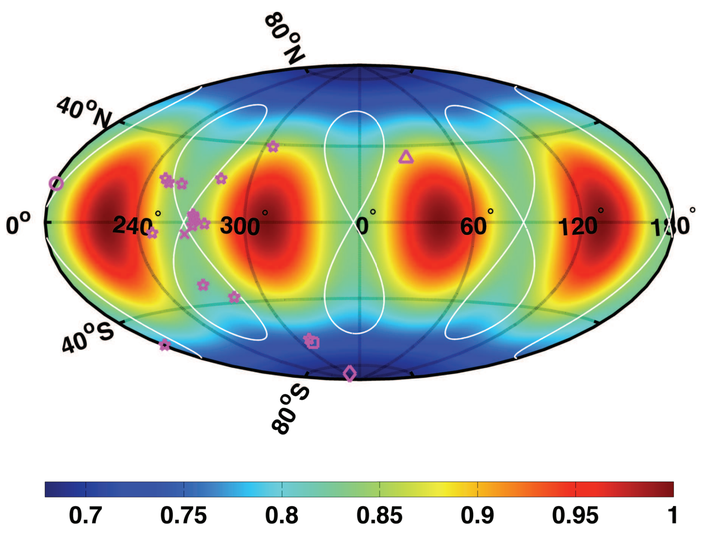

Figure 3: Color map showing $\widehat{\rho^2}$ as a function of $\boldsymbol{n}$ when the orientation is chosen to minimize sensitivity to the Galactic Center (marked by $\times$). Sources from Table 1 are indicated by the following: Globular clusters are stars, M31 is a triangle, the LMC is a square, the SMC a diamond, and the Virgo cluster is an open circle.

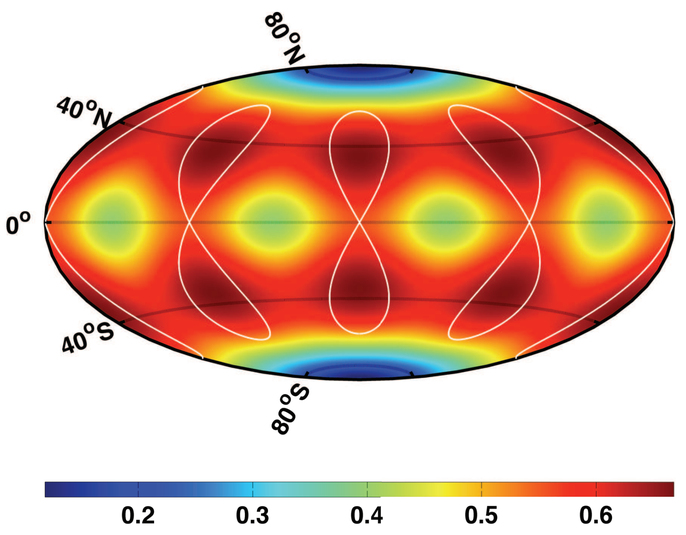

Figure 4: The fractional rms variation of $d\rho^2/dt$ from its mean value over an orbital period. The white lines trace out the paths of the nulls.

Table 1: Here is shown the ratio $\widehat{\rho^2}_{\mathrm{min}}/\widehat{\rho^2}_{\mathrm{max}}$. The Sources column abbreviations are DWD for double white-dwarf binaries, COB for compact object (neutron star or stellar mass black hole) binaries, and EMRI for extreme mass-ratio inspiral systems.

Object	Lon	Lat	Sources	$\widehat{\rho^2}_{\mathrm{min}}/\widehat{\rho^2}_{\mathrm{max}}$
Gal. Cen.	266.85172	-5.6076736	DWD, COB	0.84
Virgo Cluster	181.04266	14.333893	COB, EMRI	0.82
LMC	312.50989	-85.351425	COB	1.00
SMC	312.08823	-64.605469	COB	0.99
Androm. Gal. (M31)	27.849274	33.349022	COB, EMRI	1.04
NGC104 (47Tuc)	311.25247	-62.352768	DWD, COB	1.03
NGC3201	181.36612	-51.539581	DWD, COB	0.97
NGC6121 (M4)	248.48676	-4.8687668	DWD, COB	0.96
NGC6218 (M12)	250.57292	20.272308	DWD, COB	0.97
NGC6259 (M10)	253.45894	18.441391	DWD, COB	0.94
NGC6366	261.54391	18.122971	DWD, COB	0.88
NGC6397	266.69220	-30.290436	DWD, COB	0.90
NGC6544	271.66437	-1.5686417	DWD, COB	0.83
2MS_GC01	271.97073	3.5952682	DWD, COB	0.83
2MS_GC02	272.24817	2.6416550	DWD, COB	0.83
Terzan12	272.82751	0.66725922	DWD, COB	0.84
NGC6656 (M22)	278.31403	-0.72771454	DWD, COB	0.86
GLIMPSE01	283.12085	21.387779	DWD, COB	0.91
NGC6752	281.02106	-37.221313	DWD, COB	0.95
NGC6838 (M71)	305.34909	38.792225	DWD, COB	1.05

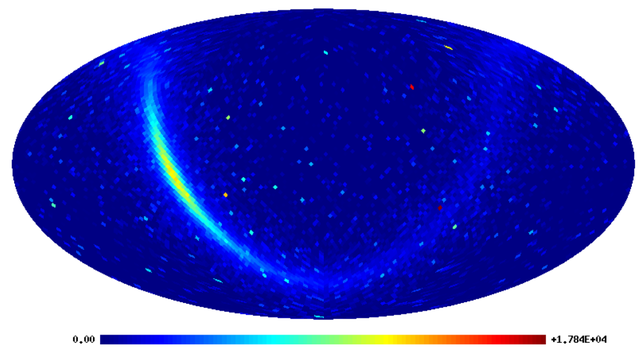

Figure 5: The directional source of confusion noise below 1 mHz from white dwarf binaries in the Galaxy.

Pointing the Detector

As the detector executes its three periodic motions about Sol during a year, the four nulls trace out figure-8 patterns on the sky. In ecliptic coordinates, these figure-8s lie within 60° of the ecliptic equator. The choice of the initial orientation of the constellation determines the ecliptic longitude for the figure-8s—for a given orientation, rotating the constellation by ϕ_0 in the detector plane corresponds to a shift in ecliptic longitude by the same angle. Thus, we can point LISA to select four regions on the sky to which it will be relatively insensitive and four regions with increased sensitivity. The sky sensitivity for a particular choice that minimizes sensitivity to the Galactic Center is shown in Fig. 3. The variation in $d\rho^2/dt$ also depends on the initial orientation of LISA, which can influence the size of the error box on the sky for individual sources. This variation is shown in Fig. 4. The phasing of these variations can also be used to enhance instantaneous sensitivity to certain regions in the sky while suppressing sensitivity in other regions—see Fig. 6 for examples of the instantaneous sensitivity toward the Galactic Center and the simultaneous instantaneous sensitivity to the Virgo Cluster.

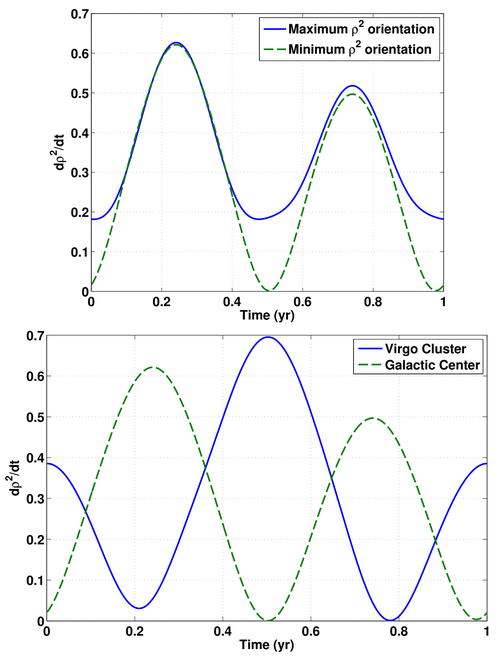

Figures 6: Top: Instantaneous sensitivity to sources in the Galactic Center for orientations chosen to maximize or minimize annual sensitivity to the Galactic Center.
Bottom: Instantaneous sensitivity to sources in the Virgo Cluster and the Galactic Center for orientations that minimize sensitivity to the Galactic Center.

Acknowledgements: MJB and LSF acknowledge the hospitality of the Aspen Center for Physics, supported by the National Science Foundation under Grant No. 1066293. KJ and LSF acknowledge the support of NSF awards 0940924 and 0969857. MJB acknowledges the support of NASA grant NNX08AB74G and the Center for Gravitational Wave Astronomy, supported by NSF Cooperative Agreements HRD-0734800 and HRD-1242090.